Available online at www.sciencedirect.com

ScienceDirect

Trans. Nonferrous Met. Soc. China 23(2013) 193−200

Transactions of Nonferrous Metals Society of China

www.tnmsc.cn

Microscopic phase-field study on directional coarsening mechanism caused by interaction between precipitates in Ni−Al−V alloy

Kun YANG, Zheng CHEN, Yong-xin WANG, Xiao-li FAN

State Key Laboratory of Solidification Processing, Northwestern Polytechnical University, Xi'an 710072, China

Received 29 December 2011; accepted 12 March 2012

Abstract: A microscopic phase-field model was used to investigate a directional coarsening mechanism caused by the anisotropic growth of long period stacking and different effects of phases on precipitation in Ni−Al−V alloy. The results show that DO_{22} mainly coarsens along its short axis, which may press the neighboring $L1_2$, leading to the interaction among atoms. Diffusion channels of Al are formed in the direction where the mismatch between γ' and γ reduces; the occupation probabilities are anisotropic in space; and direction coarsening of $L1_2$ occurs finally. With a rise of ageing temperature, phases appear later and DO_{22} is much later at a higher temperature, the average occupation probabilities of Al and V reduce, and Al changes more than V.

Key words: nickel-based alloys; microscopic phase-field simulation; directional coarsening; anisotropic growth; mismatch; diffusion

1 Introduction

γ' ($L1_2$) is the main strengthened phase of nickel-based superalloys which have significantly raised operating temperature and efficiency due to their excellent properties in service, and it may form oriented growth when stress exists [1−5]. Rafting is the oriented growth of phases, which is caused during the diffusion of elements. Stress may induce elements to diffuse in a certain direction and form diffusion channels, where new precipitates occur or disappear at the same time.

Nickel-based superalloys are a kind of alloys with negative mismatch. External load may reduce the elastic mismatch energy in a direction, which becomes a driving force of directional coarsening [6]. Therefore, mismatch stress plays an important role in directional coarsening and diffusion channels.

The mismatch of various nanosize phases, elasticity modulus and anisotropy factors, which relates to directional diffusion and rafting, may change with precipitation environments such as temperature, constituent, and crystal structures[7−9]. CAHN and HILLIARD [10] calculated the minimum energy on a coherent interface and investigated the influence of elastic energy on an even elastic system. JOHNSON and BROWN [11] and VOORHEES et al [12] investigated a heterogeneous elastic system, especially in the nano stress field. Moreover, directional diffusion caused with stress, anisotropic growth of the γ' phase, and so on were reported more in this field [13−15]. The oriented growth of γ' without stress is also found in the experiment of CMSX−4 alloy [16]. In this experiment, the elements Re and W which have larger atomic radii are added to the system, and the phases with different crystal structures form. Stress affects elements differently for these phases, which promotes or blocks the diffusion in a certain direction, and diffusion channels may be strengthened or weakened [17,18]. Therefore, new precipitates form or disappear in a direction and directional coarsening forms.

According to the phase diagram, γ' and θ phases (γ' is a short period stacking phase with a face-centered cubic lattice structure ($L1_2$), and θ is long period stacking with a tetragonal structure (DO_{22})) exist in $Ni_{75}Al_xV_{25-x}$ system in certain precipitation environments. Phases may affect each other at the interfaces during the coarsening as a reason of the anisotropic growth for the different crystal structures, and the directional diffusion may also be formed without external load. It is of interest to investigate the mechanism of directional diffusion and coarsening by the interaction between phases during the precipitation process, which incudes many factors such

---

Foundation item: Projects (51075335, 10902086, 50875217) supported by the National Natural Science Foundation of China; Project (JC201005) supported by the Northwestern Polytechnical University Foundation for Fundamental Research, China; Project (CX201007) supported by the Doctorate Foundation of Northwestern Polytechnical University, China

Corresponding author: Kun YANG; Tel: +86-29-88486023; E-mail: yangkunlo@126.com

DOI: 10.1016/S1003-6326(13)62446-2

as elements, precipitation order, components, temperautre, crystal strucutres and mismatch. It is difficult to describe and analyze this process with the tranditional ways because this is a high-concentration gradient non-linear nonequilibrium stage with various complex overlopping process such as atom clustering, spinodal decomposition, nucleation, disordered-order transition, growth and coarsening.

2 Model and method

The microscopic phase-field kinetics model created by KHACHATURYAN [19] and developed by CHEN et al [20] is a kind of phase-field method, which uses atom transition probability (occupation probability) of the lattice as the field variables to describe the microstructure evolution, and it is a discrete lattice form of Cahn-Hilliard diffusion equation [10]. The functions of this model are at atomic scale so that we can obtain the information about atomic coordinates and organizational structures during the precipitation process. The information about the atoms for the system at different time can be used to describe the complex processes such as atom clustering, ordering, interface migration and coarsening. Theoretically, it is better to study the diffusion process and the dendritic growth by this method [21].

$$\begin{cases} \dfrac{\mathrm{d}P_{\mathrm{A}}(r,t)}{\mathrm{d}t}=\dfrac{1}{k_{\mathrm{B}}T}\cdot\sum\limits_{r'}\left[L_{\mathrm{AA}}(r-r')\dfrac{\partial F}{\partial P_{\mathrm{A}}(r',t)}+\right. \\ \left. L_{\mathrm{AB}}(r-r')\dfrac{\partial F}{\partial P_{\mathrm{B}}(r',t)}\right]+\xi(r,t) \\ \dfrac{\mathrm{d}P_{\mathrm{B}}(r,t)}{\mathrm{d}t}=\dfrac{1}{k_{\mathrm{B}}T}\cdot\sum\limits_{r'}\left[L_{\mathrm{BA}}(r-r')\dfrac{\partial F}{\partial P_{\mathrm{A}}(r',t)}+\right. \\ \left. L_{\mathrm{BB}}(r-r')\dfrac{\partial F}{\partial P_{\mathrm{B}}(r',t)}\right]+\xi(r,t) \end{cases} \tag{1}$$

Equation (1) is a microscopic Langevin equation, where $L_{\alpha\beta}(r\!-\!r')$ is the atom transition probability constant of α and β, which changes from lattice r to r'; and α, β =A, B or C; $\xi(r, t)$ is thermal noise random phase; k_{B} is Boltzmann constant; t is time step; T is the temperature; $P_{\mathrm{A}}(r, t)$, $P_{\mathrm{B}}(r, t)$ and $P_{\mathrm{C}}(r, t)$ stand for occupation probability of A,B and C at a certain time step, and $P_{\mathrm{C}}(r, t)= 1-P_{\mathrm{A}}(r, t)-P_{\mathrm{B}}(r, t)$; F is the free energy of system, it comes from the mean field theory that

$$F=(1/2)\sum_{\boldsymbol{r}}\sum_{\boldsymbol{r}'}W(r-r')P(r')P(r')+K_{\mathrm{B}}T\cdot \sum_{r}[P(r')\ln P(r')+(1-P(r'))\ln(1-P(r'))] \tag{2}$$

$$W_{\alpha\beta}(r-r')=W_{\alpha\beta}(r-r')_{\mathrm{ch}}+W_{\alpha\beta}(r-r')_{\mathrm{el}} \tag{3}$$

where $W_{\alpha\beta}(r-r')$ is a useful interaction energy among atoms and in the Fourier space is $V(k)$; $W_{\alpha\beta}(r-r')_{\mathrm{el}}$ is the elastic interaction energy and in Fourier space is $B(e)$; $W_{\alpha\beta}(r-r')_{\mathrm{ch}}$ is the chemical interaction energy and in Fourier space is $V(k)_{\mathrm{ch}}$.

$$V(k)=V(k)_{\mathrm{ch}}+B(e) \tag{4}$$

The elastic mismatch stress is then added to the free engergy expression.

$$B(e)=-\frac{4(c_{11}+2c_{12})}{c_{11}(c_{11}+c_{12}+2c_{44})}\varepsilon_0^2(c_{11}-c_{12}-2c_{44})\cdot \left[\frac{h^2k^2}{(h^2+k^2)^2}-0.125\right] \tag{5}$$

where c_{ij} is the elastic constant of alloy and the used lattice constant is from Ref. [22]; the mismatch between γ' and γ is from Ref. [23] and the mismatch between θ' and θ is from Ref. [24].

A Fourier transform was applied to Eqs. (1) and (2) and the free energy was added to the microscopic Langevin equation in the Fourier space. We solved the equation using the Euler method and obtained the occupation probabilities of the atoms at different time steps, and the evolution of morphologies for precipitates is obtained according to the variation of occupation probabilities.

We chose 128×128 lattice points and used dark blue for the Ni atoms, light green for the Al atoms and red for the V atoms. The lattice points are dark blue if the occupation probability value of Ni is 1, light green if the value of Al is 1 and red if the value of V is 1. The depth of color defined the height of the value for an atom at a lattice point. The figures for the precipitation process are obtained to investigate and analyze the diffusion process and the dendritic growth.

3 Results and discussion

3.1 Evolution of directional coarsening and structures of phases

Figure 1 shows the crystal structures of order phases and morphology of precipitates which separate from matrix when t=2.2×10^4. L1$_2$ is a face-centered cubic structure with eight Al atoms and six Ni atoms in a lattice. Ni atoms occupy six face-centered positions, which are shown as dark blue. Al atoms occupy eight vertices, which are shown as light green in the simulation figure. DO$_{22}$ is a long-period stacking order structure (LPS), which is a face-centered tetragonal structure with fourteen Ni atoms and nine V atoms in a lattice. Ni atoms occupy ten face-centered positions and four vertices of the middle crystal face, which are shown as dark blue in the simulation figure. V atoms occupy eight vertices and the body centered position, which are shown as red. In Fig. 1, $L1_2$ precipitates appear firstly and occupy most of the figure, and a few DO_{22} forms at the boundary of $L1_2$.

As the time goes, the grains of DO_{22} become more, and precipitates do not arrange in neat rows at *t* of 40000, which shows a weaker tendency of directional coarsening (Fig. 2(a)). At $t=8\times10^4$, grains of DO_{22} become larger and DO_{22} phases coarsen more, and $L1_2$ becomes smaller at the same time (Fig. 2(b)). In Fig. 2(c), precipitates become shorter along [100] and more elongated along [001]. At $t=10.5\times10^5$, the tendency of directional coarsening becomes stronger (Fig. 2(d)). In Fig. 3, DO_{22} grows mainly along its short axis, and the neighboring $L1_2$ phases disappear along the same direction. According to this evolution, we can thus obtain that it is the process that $L1_2$ appears firstly with

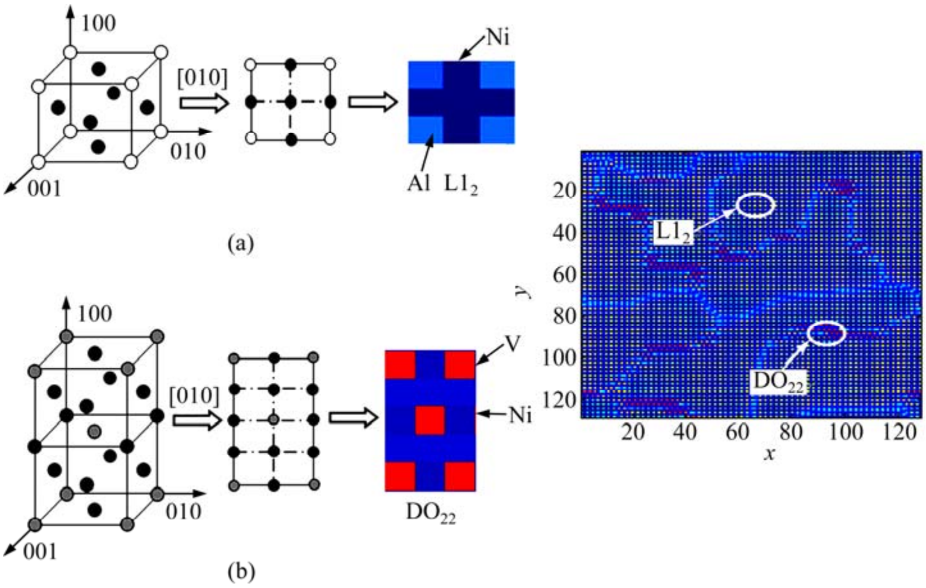

Fig. 1 Morphology of $Ni_{75}Al_{6.7}V_{18.3}$ alloy at 1100 K when $t=2.2\times10^4$ and corresponding relation between simulation results and lattice structures projected in direction [010] (Horizontal and ordinate coordinates are lattice positions in [001] and [100], respectively): (a) Ni_3Al-L1_2; (b) Ni_3V-DO_{22}

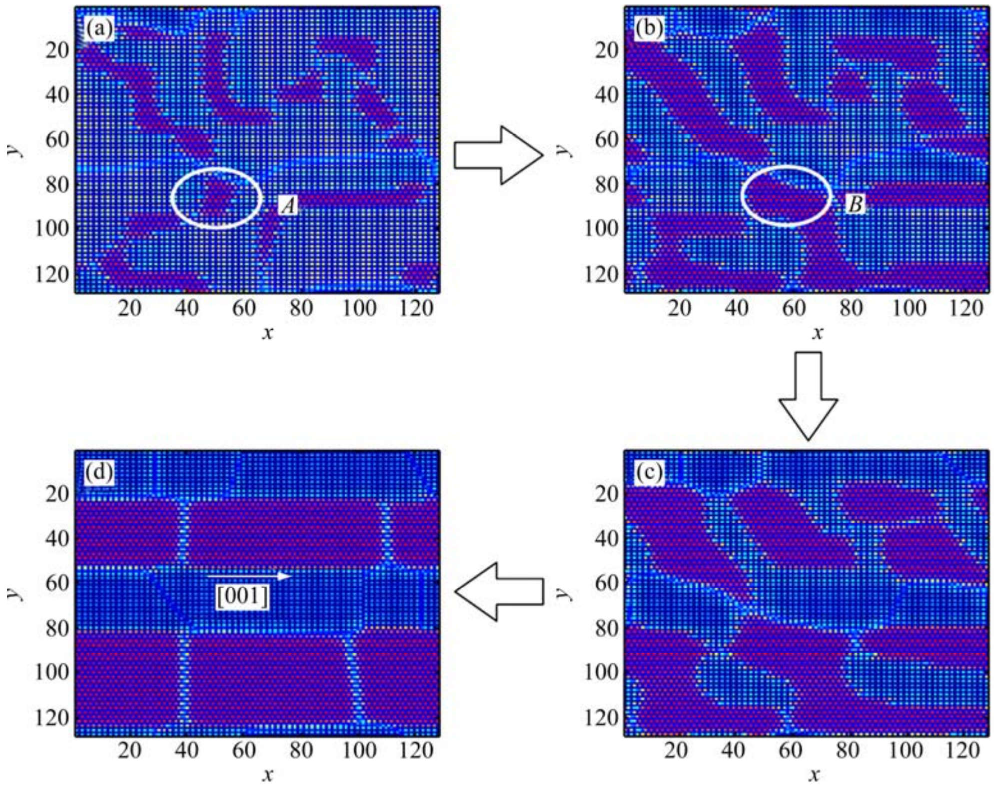

Fig. 2 Evolution of morphology for $Ni_{75}Al_{6.7}V_{18.3}$ alloy at 1100 K at different time steps (Horizontal and ordinate coordinate are lattice positions in [001] and [100], respectively): (a) $t=4\times10^4$; (b) $t=8\times10^4$; (c) $t=3\times10^5$; (d) $t=10.5\times10^5$

isotropic growth so that the tendency of directional coarsening is weaker at the beginning, and DO_{22} forms at the boundary of $L1_2$ and coarsens along a certain direction to influence the growth of $L1_2$, and directional coarsening of precipitates occurs finally.

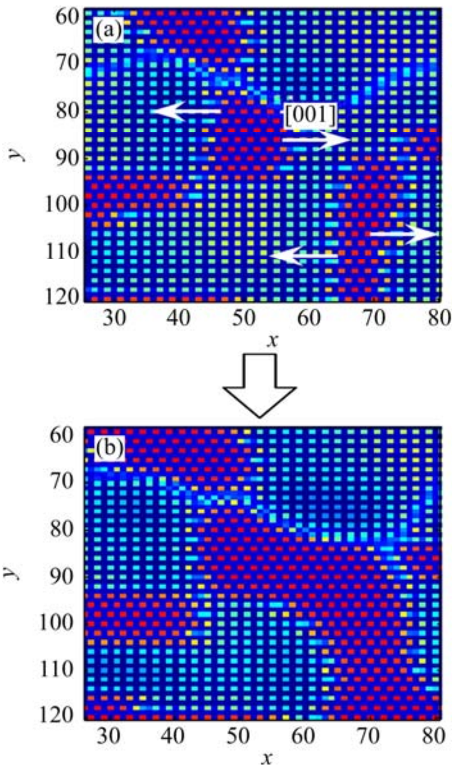

Fig. 3 Evolution of oriented growth for DO_{22} from t of 4×10^4 (a) to 8×10^4 (b)

3.2 Directional coarsening caused by influence of migration between phases

In order to study the mechanism of directional coarsening between phases, structures of the interface between two phases and the occupation probabilities of atoms in these positions were investigated (Fig. 4). DO_{22} coarsens along the direction [001] in Fig. 3, and the structures of interface between $L1_2$ and DO_{22} precipitates are shown in Figs. 4(a) and (b). In position *a*, the occupation probability of Ni reduces and that of V rises, and Al changes little in Fig. 4(c). In position *b*, the occupation probability of Al and V reduces and that of Ni increases, and Al reduces more than V (Fig. 4(d)). In position *e*, the occupation probability of Al reduces and that of V increases, and Ni changes few (Fig. 4(e)). This indicates that during the process, Ni atom turns to V in position *a*, Al atom turns to Ni in position *b*, and Al atom turns to V in position *e*. Therefore, DO_{22} prefers to coarsen along its short axis (the direction of [001]).

Figure 5 shows the evolution of occupation probabilities of Al for $L1_2$ in [100] and [001]. At t=50000, occupation probabilities of Al in center are higher than those in the boundary for $L1_2$ phase in [001]. As time goes on, occupation probability of Al rises and reaches balance little by little. However, occupation probability of Al rises more in the boundary in [001] during this process (Fig. 5(a)), and it changes few in the boundary in [100] at the same time (Fig. 5(b)). At $t=10.5\times10^5$, occupation probability of Al almost reaches balance in two directions, obvious anisotropic diffusion of Al occurs in spatial scale, the diffusion of Al is blocked in [100] and promoted in [001], and directional coarsening occurs. Nickel-based superalloys are a kind of alloys with negative misfit. If a tensile stress exists in [100], γ' precipitates are compressed by neighboring phases, and the elastic misfit energy between γ' and matrix reduces in [001], where Al atoms from matrix diffuse and concentrate easily. Al atoms enter γ' from the [001] direction so that new $L1_2$ forms, and thus directional coarsening forms finally. Moreover, with a compressive stress in [100], $L1_2$ precipitates are compressed in [100], where the elastic misfit energy reduces, and thus they coarsen along this direction. Without external load, the neighboring $L1_2$ is also compressed with the anisotropic growth of DO_{22}, the mismatch between $L1_2$ and matrix may reduce in a direction, the release of mismatch energy gives a drive of directional diffusion for Al atoms so that their occupation probabilities change in a direction, and directional coarsening occurs finally.

3.3 Effects of phases

3.3.1 Effects of phases on precipitates

In this work, $L1_2$ separates from matrix first. However, the anisotropic growth of DO_{22} makes the neighboring $L1_2$ form diffusion channels later, and the occupation probability of Al may be later balance. In Fig. 4(c), Ni transforms to V in position *a*, where few Al takes part in, and the occupation probability of Al is lower. In Fig. 4(d), Al transforms to Ni in position *b*, where a higher occupation probability of V exits at the beginning. In Fig. 4(e), Al transforms to V in position *e*, where a higher occupation probability of Ni exits. Ni and V atoms have a higher occupation probability than Al atoms during the coarsening process of DO_{22}.

In Fig. 6, the occupation probabilities of V almost reach the constant values (y=0.8704) when $t=5.167\times10^4$, and Al reaches balance (y=0.6296) when $t=5.565\times10^5$. V atoms have a higher occupation in DO_{22} phase and the values are earlier to reach constant than Al in $L1_2$. In the system of $Ni_{75}Al_{6.7}V_{18.3}$, the component of V is much higher than Al in the alloy, and thus the occupation probability of V is higher. DO_{22} occurs later, and its anisotropic growth causes the neighboring $L1_2$ to be

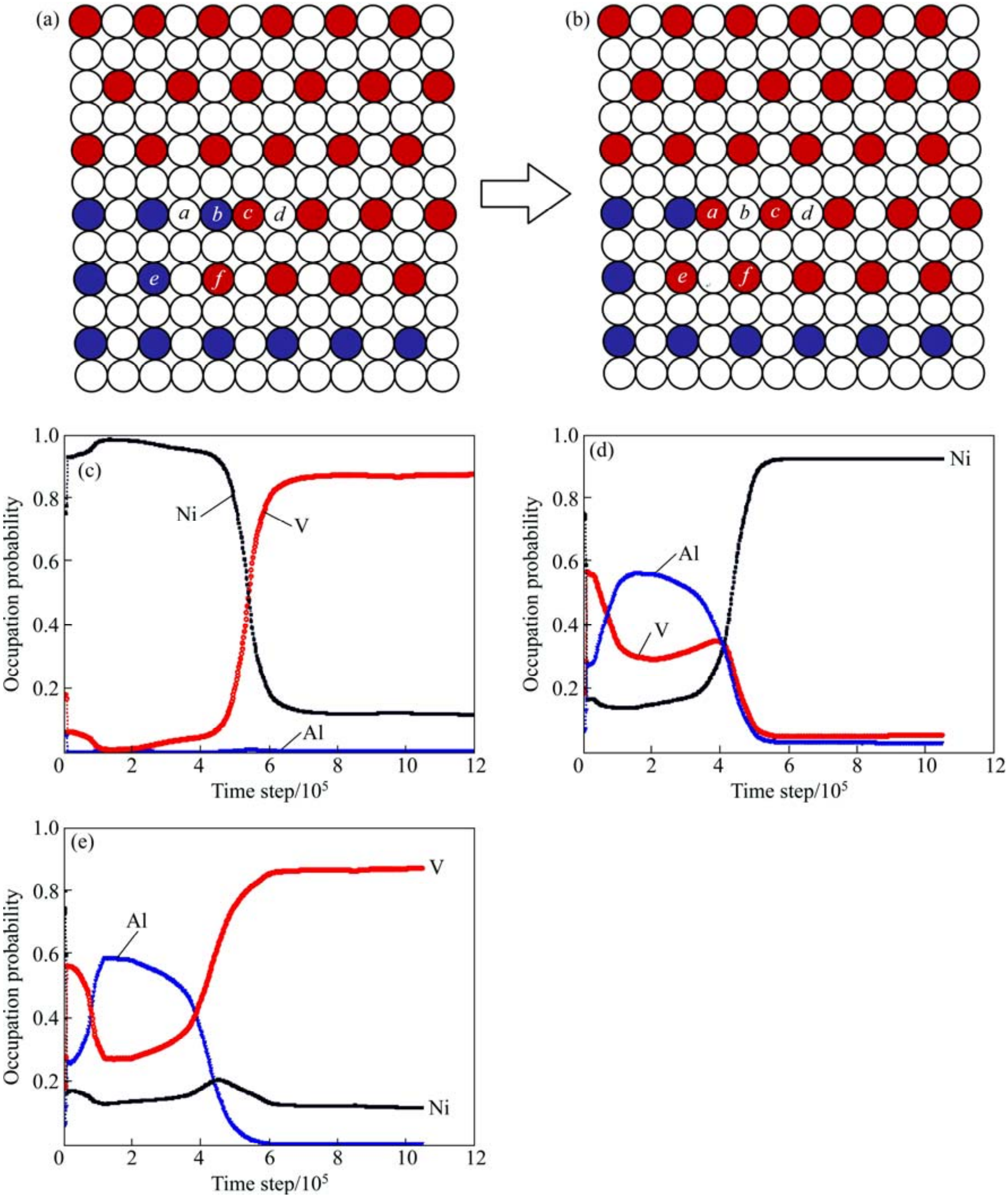

Fig. 4 Evolution of interface between L1$_2$ and DO$_{22}$ (a,b) and occupation probabilities of atoms at interface in positions *a* (c), *b* (d) and *e* (e)

pressed. The mismatch increases or reduces in a direction as a result that it gives a drive of directional diffusion of Al, which makes diffusion channels of Al and directional coarsening of L1$_2$ form in different directions. Therefore, the occupation probability of Al is higher first than V, reduces during the directional coarsening and balances later.

3.3.2 Effects of phases on ageing temperature

Figure 7(a) shows the evolution of appearing time for L1$_2$ and DO$_{22}$ precipitates as the temperature changes from 1000 to 1140 K. The time step increases with a rise of temperature, L1$_2$ always appears earlier than DO$_{22}$, DO$_{22}$ changes more than L1$_2$, and the difference of time step between two phases increases rapidly at a higher temperature. In Fig. 7(b), the occupation probabilities of Al and V reduce with a rise of temperature, and Al (from 0.71 to 0.61) varies more than V (from 0.92 to 0.85). The rise of temperature makes the drive of nucleation for two phases weaken, two phases are harder to precipitate, and thus they appear later at a higher temperature. However,

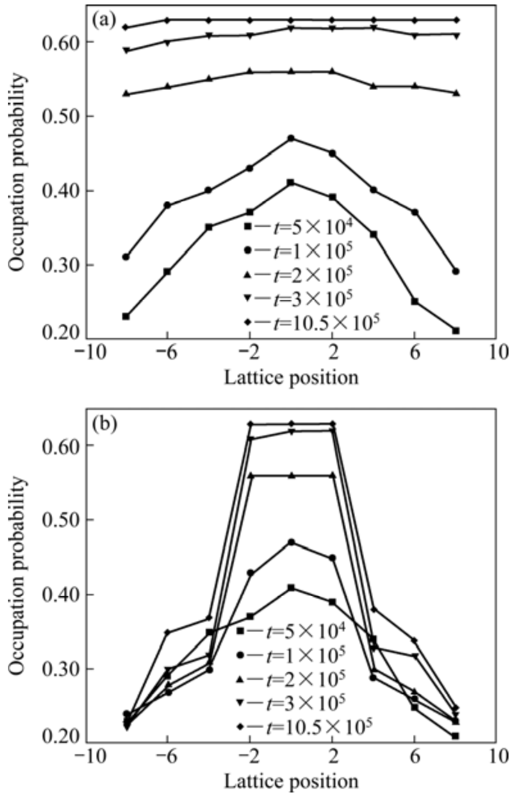

Fig. 5 Occupation probability of Al for $L1_2$ channel in two directions: (a) [001]; (b) [100]

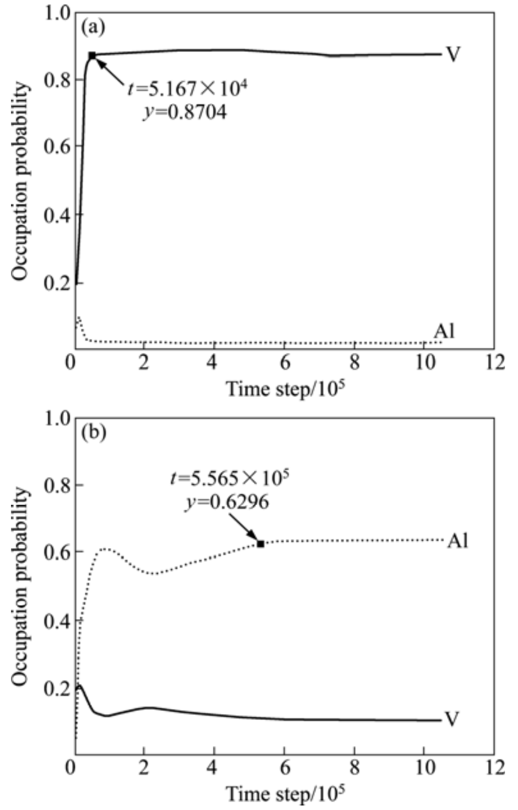

Fig. 6 Variations of average occupation probability values of Al and V in different diffusion channels: (a) DO_{22} channel; (b) $L1_2$ channel

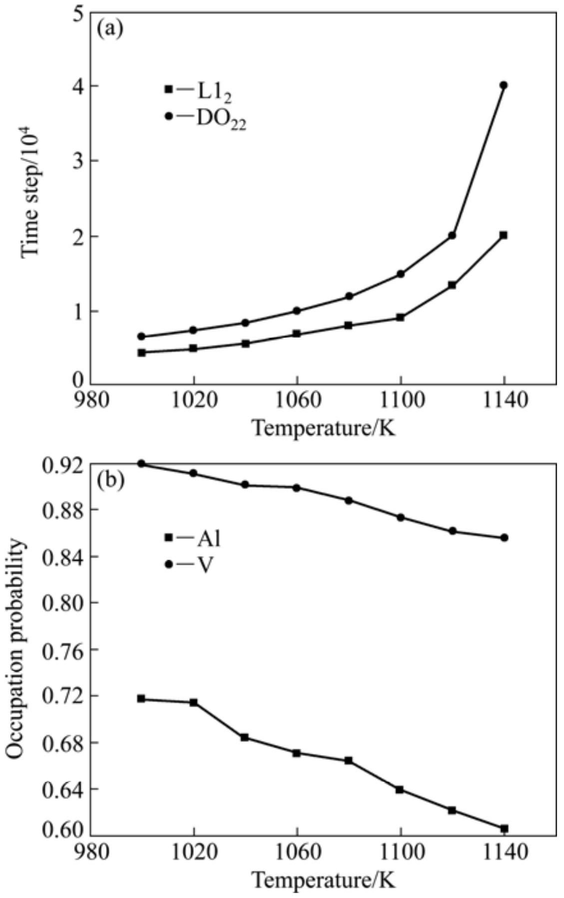

Fig. 7 Evolution of appearing time for two phases (a) and occupation probability of Al and V of $Ni_{75}Al_{6.7}V_{18.3}$ alloy (b)

the effects of phases on temperature are different, and DO_{22} may appear much later than $L1_2$ at a higher temperature. The atomic coordinate environment may affect the occupation of atoms in lattice positions. Due to the different structures for two phases, the atomic coordinate environments of V in DO_{22} and Al in $L1_2$ are different, and abilities of occupation in the lattice position are also different. Therefore, the occupation probability of V in DO_{22} is higher than Al in $L1_2$. The reducing of the drive of nucleation also makes the lower occupation probabilities for two phases at a higher temperature. DO_{22} appears much later at a higher temperature and its anisotropic growth causes the directional coarsening of $L1_2$, diffusion channels of Al are later balance, and the occupation probability of Al is also affected by the coarsening of DO_{22}, which changes more with the rise of temperature.

4 Conclusions

1) A directional coarsening mechanism caused by the interaction of anisotropic growth for LPS was studied and the different effects of phases on the interaction were

discussed by microscopic phase-field method.

2) DO_{22} grows along its short axis. It may press the neighboring $L1_2$ and reduce or increase the mismatch, which makes the interaction among atoms and forces Al to form diffusion channels in different directions, and directional coarsening of $L1_2$ occurs and rafting forms finally.

3) The occupation probabilities of Al in $L1_2$ vary differently in the directions during the coarsening process. The occupation probability of Al at the boundary of $L1_2$ rises more in [001], where $L1_2$ coarsens. However, the occupation probability of Al in the boundary changes few in [100], the occupation probability of Al is anisotropic in space, and directional coarsening of $L1_2$ occurs.

4) The effects of phases on precipitation environments are different. With the rise of temperature, two phases appear later, DO_{22} varies rapidly at a higher temperature. The occupation probability of Al and V reduces, and Al reduces more than V.

References

[1] FRATZL P, PENROSE O, LEBOWITZ J L. Modeling of phase separation in alloys with coherent elastic mismatch. [J]. Journal of Statistical Physics, 1999, 95: 1429−1503.

[2] STALLYBRASS C, SCHNEIDER A, SAUTHOFF G. The strengthening effect of (Ni,Fe)Al precipitates on the mechanical properties at high temperatures of ferritic Fe−Al−Ni−Cr alloys. [J]. Intermetallics, 2005,13: 1263−1268.

[3] NABARRO F R N. Rafting in superalloys [J]. Metall Mater Trans A, 1996, 27: 513−530.

[4] TETSU I, DAISUKE K, MASAHIKO H, KATSUSHI T, MAKOTO O, TADAHARU Y, HIROSHI H. Rafting mechanism for Ni-base superalloy under external stress: Elastic or elastic-plastic phenomena [J]. Acta Mater, 2003, 51: 4033−4044.

[5] SOCRATE S, PARKS D M. Numerical determination of the elastic driving force for directional coarsening in Ni-superalloys [J]. Acta Metall, 1993, 41: 2185−2209.

[6] ZHAO X B, LIU L, YANG C B, LI Y F, ZHANG J, FU H Z. Influence of crystal orientation on cellular growth of a nickel-base single crystal superalloy [J]. J Alloys Compd, 2011, 509: 9645−9649.

[7] VOGEL F, WANDERKA N, MATSUMURA S, BANHART J. Early stages of decomposition within the gamma' phase of a Ni−Al−Ti model alloy. [J]. Intermetallics, 2012, 22: 226−230.

[8] BRUNETTI G, SETTEFRATI A, HAZOTTE A, DENIS S, FUNDENBERGER J J, TIDU A. Determination of gamma-gamma'lattice misfit in a single-crystal nickel-based superalloy using convergent beam electron diffraction aided by finite element calculations [J]. Micron, 2012, 43: 396−406.

[9] HOSSEINI S S, NATEGH S, EKRAMI A A, Changes of gamma' precipitate characteristics in damaged superalloy IN738LC during different stages of rejuvenation heat treatment cycles [J]. Materials Science and Technology, 2012, 2: 213−219.

[10] CAHN J W, HILLIARD J E. Free energy of a nonuniform system: Interfacial free energy [J]. Chem Phys, 1958, 28: 258−267.

[11] JOHNSON R A, BROWN J R. Vacancies and antisite defects in ordered alloys [J]. Journal of Materials Research, 1992, 12: 3213−3218.

[12] VOORHEES P W, MCFADDEN G B, JOHNSON W C. On the morphological development of second-phase particles in elastically stressed solids [J]. Acta Metallurgica et Materialia, 1992, 40: 2979−2992.

[13] TIAN Su-gui, ZHOU Hui-hua, ZHANG Jing-hua, YANG Hong-cai. A directional coarsening mechanism of the γ'-phase during creep of a single crystal nickel-base superalloy [J]. Acta Metall Sin, 1998, 34: 591−596.

[14] PENG Zhi-fang, YAN Yan-hui. Phase morphology evolution and anisotropic creep behaviour of nickel-base single crystal superalloy CMSX-4 [J]. Acta Metall Sin, 1997, 33: 1147−1154.

[15] LAPIN J. Effect of directional solidification and heat treatments on the microstructure and mechanical properties of multiphase intermetallic Zr-doped Ni−Al−Cr−Ta−Mo alloy. [J]. Intermetallics, 2006, 14: 1417−1427.

[16] CHENG K Y, JOB C Y, KIMC D H, JINA T, HUA Z Q. Influence of local chemical segregation on the γ' directional coarsening behavior in single crystal superalloy CMSX-4 [J]. Materials Characterization, 2009, 60: 210−218.

[17] CABET E, PASTUREL A, DUCASTELLE F. $L1_2$-DO_{22} competition in the pseudobinary (Pt, Rh)$_3$V, Pt$_3$(V, Ti), and (Pd, Rh)$_3$V alloy: Phase stability and electronic structure. [J]. Physical Review Letter, 1996, 76: 3140−3143.

[18] TOMIHISA K, KANENOAND Y. Phase relation and microstructure in multi-phase intermetallic alloys based on Ni_3Si−Ni_3Ti−Ni_3Nb pseudo-ternary alloy system. [J]. Intermetallics, 2004, 12: 317−325.

[19] KHACHATURYAN A G. Theory of structural transformation in solids [M]. New York: Wiley, 1983: 129.

[20] CHEN L Q, KHACHATURYAN A G. Computer simulation of decomposition reactions accompanied by a congruent ordering of the second kind [J]. Scripta Metallurgica et Materialia, 1991, 25: 61−66.

[21] WANG Y, KHACHATURYAN A G. Shape instability during precipitate growth in coherent solids [J]. Acta Metall Mater, 1995, 43: 1837−1845.

[22] PRIKHODKO S V, CARNES J D, SAAK D G, ARDELL A J. Elastic constants of a Ni−12.69 at.% Al alloy from 295 to 1300 K [J]. Scr Mater, 1997, 38: 67−75.

[23] MIYAZAKI T, IMAMURA M, KOZATI T. The formation of " γ' precipitate doublets " in Ni−Al alloys and their energetic stability [J]. Mater Sci Eng, 1982, 54: 9−17.

[24] SINGH J B, SUNDARARAMAN M, BANERJEE S, MUKHOPADHYA P. Evolution of order in melt-spun Ni−25at.%V alloys [J]. Acta Mater, 2005, 53 :1135−1143.

微观相场法研究镍基合金沉淀相间作用的定向粗化机制

杨 坤，陈 铮，王永欣，范晓丽

西北工业大学 凝固技术国家重点实验室，西安 710072

摘　要：采用微观相场法研究 Ni−Al−V 合金中由长周期沉淀相各向异性生长所引起的定向粗化机制以及沉淀过程对有序相的不同作用。结果表明：DO_{22} 相主要沿着其短轴方向粗化，挤压相邻的 $L1_2$ 相并导致原子间的相互作用，使其与基体间的错配发生变化，并在特定方向上释放出配错能，形成 Al 原子的扩散通道，引起其原子占位在空间上的各向异性，最终导致 $L1_2$ 相定向粗化。随着时效温度的升高，两相的析出滞后，而 DO_{22} 相在较高温度的滞后更为显著；Al 和 V 的平均占位几率降低，且 Al 降低得较多。

关键词：镍基合金；微观相场模拟；定向粗化；各向异性生长；错配；扩散

(Edited by Xiang-qun LI)